



# MALIGNANT HEPATIC TUMORS IN PEDIATRIC PATIENTS: CLINICAL AND RADIOLOGICAL FEATURES

M.L. GIUNTA<sup>1</sup>, F. ROCCASALVA<sup>1</sup>, G. ATTINÀ<sup>1</sup>, G. CAPPELLO<sup>1</sup>,  
V. DI BENEDETTO<sup>2</sup>, M.G. SCUDERI<sup>2</sup>, G. BELFIORE<sup>1</sup>, A.G. MUSUMECI<sup>1</sup>,  
P.V. FOTI<sup>1</sup>, A. DI CATALDO<sup>3</sup>, G. PETRILLO<sup>1</sup>, L. SALVATORELLI<sup>4</sup>, S. PALMUCCI<sup>1</sup>

<sup>1</sup>Radiodiagnostic and Radiotherapy Unit, University Hospital "Policlinico-Vittorio Emanuele", Catania, Italy.

<sup>2</sup>Department of Pediatric Surgery, University Hospital "Policlinico-Vittorio Emanuele", Catania, Italy.

<sup>3</sup>Pediatric Hematology and Oncology Unit, University Hospital "Policlinico-Vittorio Emanuele", Catania, Italy.

<sup>4</sup>Department of Medical and Surgical Sciences and Advanced Technologies, G.F. Ingrassia, University Hospital "Policlinico-Vittorio Emanuele", Anatomic Pathology Section, University of Catania, Catania, Italy.

**Abstract:** *Hepatic tumors represent only 1% of all pediatric neoplasms; unfortunately, in two-thirds of cases, they are malignant. Clinical presentation is often non-specific, causing late diagnosis.*

*Imaging plays a fundamental role in characterizing lesions, staging and evaluating the adequate treatment and the outcome. For staging disease, The Pretreatment Extent of Disease (PRETEXT) system could be assessed using Computed Tomography (CT) or Magnetic Resonance (MR).*

*Main malignant liver tumors include: hepatoblastoma, hepatocellular carcinoma, fibrolamellar carcinoma, undifferentiated embryonal sarcoma, rhabdomyosarcoma, epithelioid hemangioendothelioma, hepatic lymphoma, angiosarcoma, liver metastases.*

*Clinical and radiological features of these neoplasms are briefly reported in this pictorial review, emphasizing morphological signs observed with ultrasonography, computed tomography and magnetic resonance. However, the diagnosis could not be easy, because the majority of tumors is very often heterogeneous in appearance. A multidisciplinary approach is recommended, in order to make a correct diagnosis and help clinicians in management of patients.*

**Keywords:** *Hepatic neoplasms, Imaging, Clinical and radiological features.*

## INTRODUCTION

Liver tumors account for roughly 1% of all pediatric neoplasms and, in two-thirds of cases, they are malignant<sup>1,2</sup>. Among primary hepatic neoplasms in children, epithelial (hepatocyte-derived) tumors are more common than the mesenchymal ones<sup>3</sup>.

Clinical presentation is relatively uniform with abdominal enlargement; unfortunately, specific

symptoms develop late. A differential diagnosis of liver tumors in children can be obtained considering some factors, such as the age of the child, clinical information, laboratory tests (especially AFP) and imaging findings.

Imaging plays a fundamental role in characterizing lesions, staging and evaluating the adequate treatment and the outcome. Although the radiological findings of some tumors can overlap, knowledge



of the specific US, CT and MR imaging features of each malign liver tumor is helpful to assess the correct diagnosis. In addition, in pediatric radiology the risk of radiation exposure and sedation must be carefully evaluated, and an integrated approach using different modalities is often mandatory.

Ultrasonography (US) represents the first-level imaging modality in a child with suspected abdominal mass because of its lack of ionizing radiation and no need for sedation. Of course the finding of a hepatic tumor is an indication for further imaging evaluation<sup>3,4</sup>.

Multidetector Computed Tomography (MD-CT) is an important technique for the preoperative planning of treatment for patients with malignant neoplasms of the liver. The standard CT approach tends to use relatively low-dose techniques and to avoid unenhanced and multiphase images<sup>5,6</sup>.

MR provides multiplanar imaging and very high contrast resolution on images, without any ionizing radiation exposure. On the other hand, it requires long image acquisition time and patient collaboration (breath-hold, etc); breath-hold acquisition may not be possible in the case of sedated patients, and dedicated software (navigator, respiratory-triggered acquisition) is needed in order to maintain high quality of images<sup>7</sup>. According to Kolbe et al<sup>8</sup>, the use of hepatocyte-specific contrast agents can be useful to characterize liver lesions in pediatric patients.

Aim of this pictorial review is to describe the main clinical and radiological features of a malignant hepatic tumor. For each lesion, after a brief summary of clinical features, we provide radiological descriptions in order to increase knowledge of imaging features of these malignant hepatic diseases.

## PRETEXT SYSTEM

The Pretreatment Extent of Disease (PRETEXT) system, designed by the International Childhood Liver Tumor Strategy Group (SIOPEL) and up-

**Table 1.** The Pretreatment Extent of Disease (PRETEXT) system<sup>5,9-11</sup>, for staging pediatric liver malignancies.

PRETEXT number	Definition
I	One section is involved and three adjoining sections are free
II	One or two sections are involved, but two adjoining sections are free
III	Two or three sections are involved, and no two adjoining sections are free
IV	All four sections are involved

dated in June 2005, is used for staging and risk stratification of liver tumors<sup>5,9-11</sup>.

The system was first developed for hepatoblastoma, and then applied to all pediatric malignant liver tumors. Using Couinaud's system of segmentation of the liver, PRETEXT number is calculated subtracting the highest number of contiguous liver segments that are not involved by tumor from four<sup>5</sup>. PRETEXT system is summarized in tables 1 and 2.

## HEPATOBLASTOMA

### Clinical features

Hepatoblastoma is the most common tumor among primary hepatic malignancy in childhood<sup>12</sup>. Risk factors include preterm birth, low-birth-weight, Beckwith-Wiedemann syndrome and Gardner syndrome<sup>3,12,13</sup>.

Analysing the epidemiology of the tumor in different regions, hepatoblastoma has been reported as the most common primary liver tumor in Western countries, whereas HCC is the most common malignant hepatic lesion encountered in Eastern regions<sup>14</sup>.

In 90% of cases it is seen in patients younger than 5 years of age, and a predominance in male of 1,7:1 is described<sup>3,14</sup>. This tumor originates from embryonic and fetal hepatocytes mixed with mesenchymal elements<sup>15</sup>.

The most frequent clinical finding is an abdominal enlargement associated with increased serum alpha-fetoprotein level in 90-95% of patients<sup>12-14</sup>. In some cases, the level of human chorionic gonadotropin can be also elevated with precocious puberty<sup>15,16</sup>. Hepatoblastoma can cause thrombosis of portal and hepatic venous structures and metastasis to regional lymph-nodes, lungs, bone and brain<sup>12</sup>. According to Agarwala, hepatoblastoma is a solitary mass in 80% of cases, but in 20% of patients it is multifocal with lung metastasis<sup>14</sup>.

### Imaging features

Imaging findings usually are variable in relation with the histologic type: epithelial (60% of cases), mixed (epithelial and mesenchymal, about 30%), and anaplastic type (10% of cases). The most common type is the epithelial one. Mixed and anaplastic types are characterized by presence of osteoid, cartilaginous or fibrous elements, and haemorrhagic and necrotic components, giving a heterogeneous appearing<sup>15,17</sup>. Recently, hepato-

**Table 2.** The Pretreatment Extent of Disease (PRETEXT) system<sup>5,9-11</sup>. Additional elements for staging malignancies, including: caudate lobe involvement, extrahepatic abdominal disease, tumor focality, tumor rupture of intraperitoneal haemorrhage, distant metastases, lymph node metastases, portal vein involvement, involvement of IVC (Inferior Vena Cava) and/or hepatic veins.

Caudate Lobe Involvement (C)	C1	Tumor involving the caudate lobe	All C1 patients are at least PRETEXT II
	C0	All other patients	
Extrahepatic abdominal disease (E)	E0	No evidence of tumor spread in abdomen	Add suffix "a" if ascites is present
	E1	Direct extension into adjacent organs or diaphragm	
Tumor focality (F)	E2	Peritoneal nodules	
	F0	Solitary tumor	
	F1	Two or more tumors	
Tumor rupture or intraperitoneal haemorrhage (H)	H0	No intraperitoneal haemorrhage	
	H1	Imaging and clinical findings of intraperitoneal haemorrhage	
Distant metastases (M)	M0	No metastases	Add suffix or suffixes to indicate location
	M1	Any metastases	
Lymph node metastases (N)	N0	No nodal metastases	
	N1	Abdominal nodal metastases	
	N2	Extra-abdominal nodal metastasis (with or without abdominal nodal metastasis)	
Portal vein involvement (P)	P0	No involvement	Add suffix "a" if intravascular tumor is present
	P1	Involvement of either the left or right branch of the portal vein	
	P2	Involvement of the main portal vein	
Involvement of the IVC and/or hepatic veins (V)	V0	No involvement	Add suffix "a" if intravascular tumor is present
	V1	Involvement of the hepatic veins	
	V2	Involvement of two hepatic veins	
	V3	Involvement of all three hepatic veins and/or the IVC	

blastoma is classified into epithelial type - which includes fetal (Figure 1), embryonal, macrotrabecular and anaplastic subtypes - and mixed epithelial/mesenchymal subtypes.

US: echogenicity and echotexture are very variable (Figures 2 to 4). Epithelial type tumor appears as a well delineated, multilobulated, and sep-

tated hypoechoic mass<sup>15</sup>. Mixed hepatoblastoma is heterogeneous with possible hypoechoic fibrotic septa, echogenic shadowing calcifications and anechoic foci of haemorrhage or necrosis within the tumor<sup>3</sup>. In a previous work by de Campo et al<sup>18</sup>, heterogeneity of tumor has been demonstrated in a study population including 8 hepatoblastomas<sup>18</sup>.

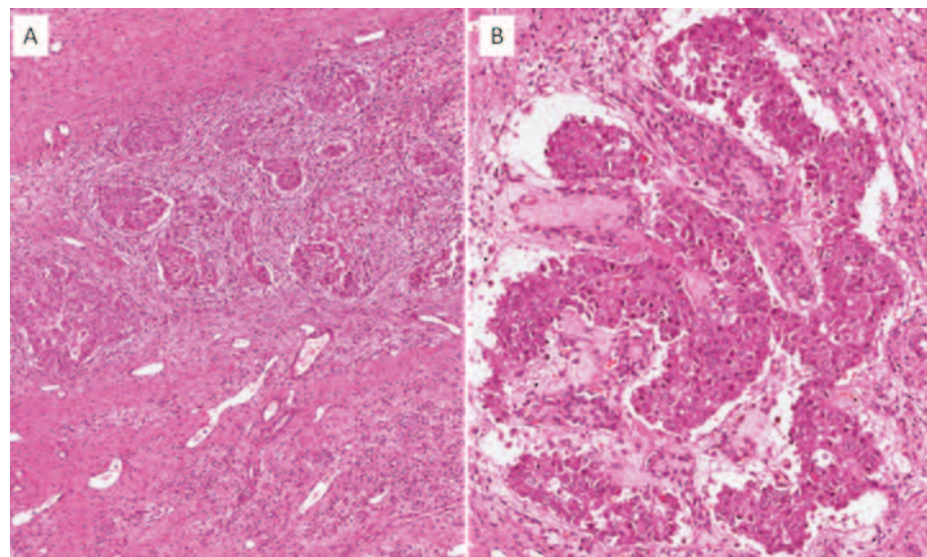


**Figure 1.** Epatoblastoma, fetal-type. A, Nests of neoplastic hepatocytes are set in a fibrous stroma (haematoxylin and eosin, original magnification, x80); B, At higher magnification, cytological details of neoplastic cells can be better appreciated (haematoxylin and eosin, original magnification, x200).

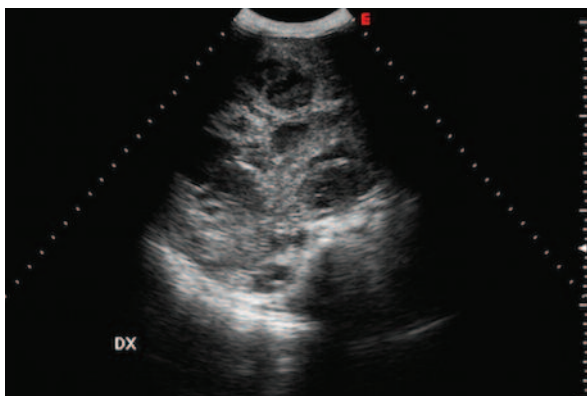


**Figure 2.** US appearance of hepatoblastoma in a 4-year-old female. The mass appears heterogeneous, with hypoechoic/anechoic nodules and fibrotic septa.

Cystic appearance of hepatoblastoma has been described by Miller<sup>19</sup>. In this case, a differential diagnosis is needed from simple hepatic cysts: generally, the presence of internal septations is helpful for assessing the correct diagnosis<sup>19</sup>.

CT: hepatoblastoma is mostly hypodense on unenhanced and contrast-enhanced images, although it is possible to find areas of enhancement, especially along the periphery and septations (Figures 5 and 6). CT scan is also the best imaging modality to detect chunky calcifications or osseous foci within the tumor<sup>12</sup>. In a series of 50 cases of hepatoblastoma retrospectively analysed, the CT pattern of calcifications and lobulations with septations has been considered a diagnostic marker to make a correct differential diagnosis, namely between hepatoblastoma and other liver neoplastic masses<sup>20</sup>.

MRI: hepatoblastoma is predominantly hypointense on T1-weighted images and hyperintense on T2-weighted sequences (Figure 7)<sup>21</sup>. MRI signal is homogeneous in the epithelial type and heterogeneous in the mixed and anaplastic pattern. After administration of contrast medium, in arterious, portal and delayed phases, hepatoblastoma demon-

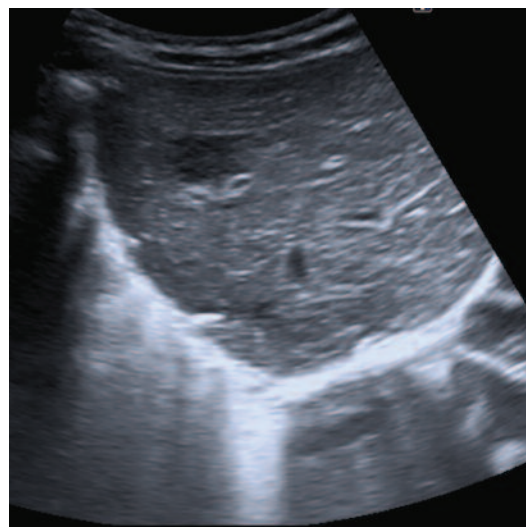


**Figure 4.** Same patient as Figure 3; 2 years after surgical treatment US exam shows a hypoechoic mass highly suspected for recurrence of hepatoblastoma. After surgical excision the hypothesis of recurrence was confirmed.

strates lower enhancement than normal liver parenchyma<sup>22</sup>. Fibrotic septa appear hypointense on both T1-weighted and T2-weighted acquisitions and enhanced after administration of gadolinium<sup>3,15</sup>. In the epatobiliary phase – acquired 20 minutes after the injection of hepatospecific agents (Gd-EOB-DTPA) – the lesion appears hypointense and sharply demarcated from the liver parenchyma<sup>23</sup>. According to a review published by Meyers, this sharp demarcation is very useful to evaluate the relationship between the tumor and the adjacent structures such as vessels and biliary tree<sup>22</sup>.

## HEPATOCELLULAR CARCINOMA

### Clinical features

HCC is the second most common tumor among primary hepatic malignancy in childhood<sup>6</sup>.

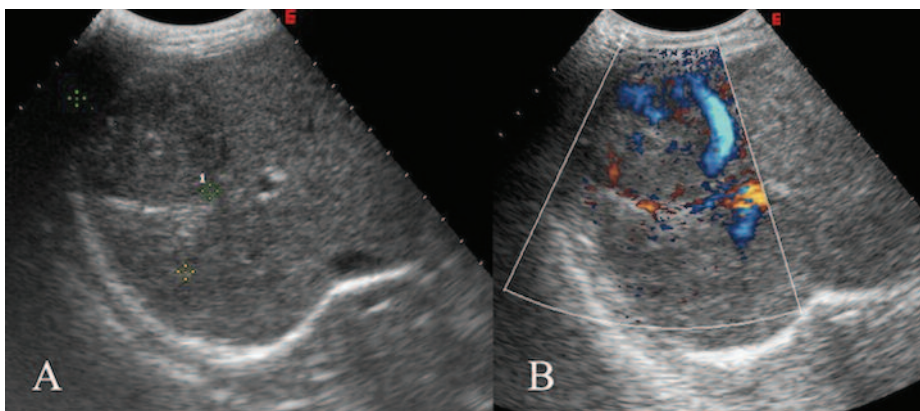


**Figure 3.** US appearance of hepatoblastoma. The lesion - located in the right liver on A - shows a slightly inhomogeneous pattern, predominantly iso/hyperechoic, with signs of vascularization on colour-US image (B).

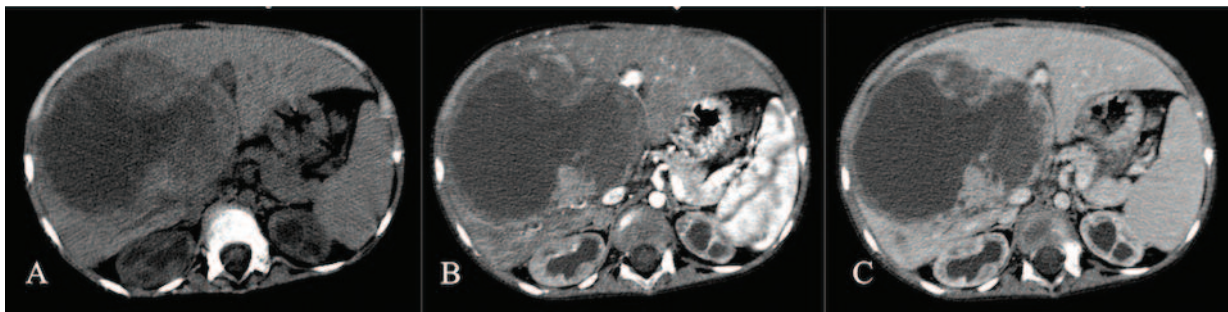


**Figure 5.** A case of hepatoblastoma in a 4-year-old female (same patient in Figure 2). A large, mostly hypodense, mass involving the right hepatic lobe is demonstrated on unenhanced CT scan (A). The lesion is characterized by the presence of a central area of fluid/necrosis and a peripheral solid part. In arterial (B) and portal (C) phases (after intravenous contrast administration), only the peripheral solid parts enhance.

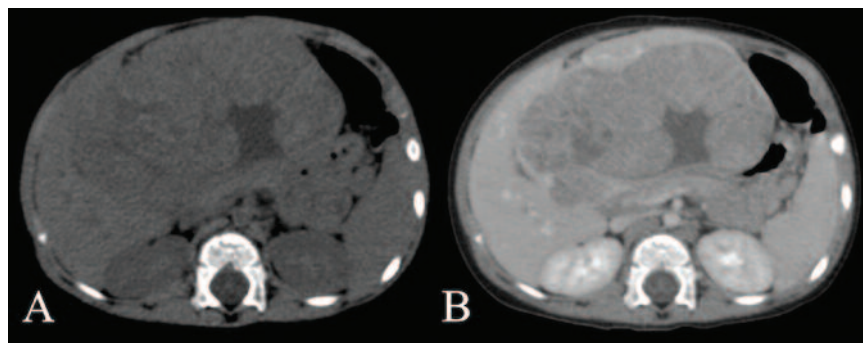


**Figure 6.** A case of hepatoblastoma in an 18-month-old child. On unenhanced CT images (A), the mass appears mostly isodense to the normal liver parenchyma with a central hypodense area. On enhanced acquisition (B), the lesion is hypodense to the enhanced normal liver parenchyma; the central area does not show any enhancement.

It usually occurs in children with hepatitis B or C infection, chronic liver disease, Wilson disease, hereditary tyrosinemia galactosemia and glycogenosis type 1<sup>3,12</sup>. In some parts of Eastern Asia and Sub-Saharan Africa, where there is a high prevalence of hepatitis B or C infection, HCC is more common than hepatoblastoma<sup>14</sup>.

Diagnosis is mostly made in children 10-14 years of age and there is a predominance in boys<sup>6</sup>. The most frequent clinical finding is an abdominal

enlargement. Abdominal pain, weight loss, anorexia or fever may be present. Blood tests typically show increased serum alpha-fetoprotein level<sup>24</sup>.

HCC can present itself as a solitary mass or can be multifocal or diffusely infiltrative, causing vascular invasion of the portal or hepatic veins or inferior vena cava<sup>12</sup>. According to the experience of Kutluk et al<sup>25</sup>, in a series of 42 cases, possible sites of metastasis are lungs, central nervous system, kidneys, bowel, right atrium and peritoneum.

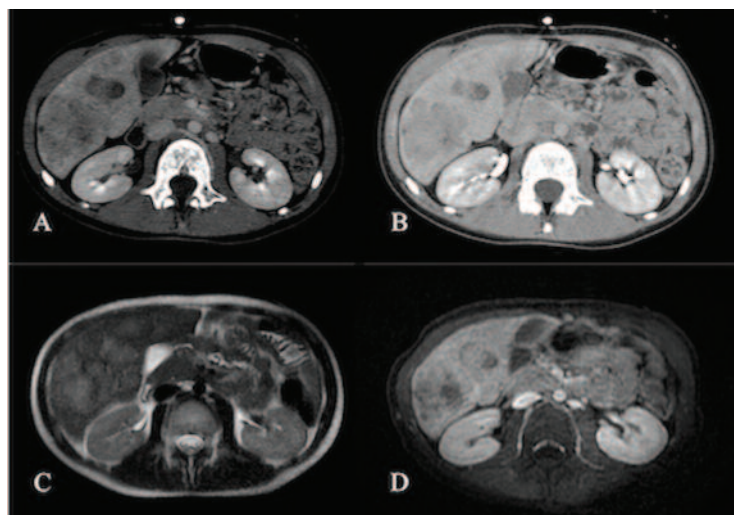


**Figure 7.** Hepatoblastoma (same patient in Figure 3). On CT scan, in portal (A) and delayed (B) phase, hepatoblastoma appears as a hypodense mass. On T2-weighted MRI (C), the lesion is slightly hyperintense. After gadolinium administration, on the portal phase (D), the mass appears hypovascular compared to normal liver parenchyma.



## **Imaging features**

Imaging features of HCC found in young patients are similar to those seen in adults<sup>12</sup>.

**US:** US appearance of HCC is variable. While small HCCs are mostly hypoechoic (even though they may be iso- or hyperechoic), larger tumors appear more heterogeneous because of the presence within the lesion of fat, necrosis or haemorrhage. Sometimes it is possible to see the tumor capsule as a thin hypoechoic halo<sup>15</sup>. Doppler evaluation shows high-velocity arterial flow<sup>6</sup>.

**CT:** HCC usually appears as an isodense or slightly hypodense mass on unenhanced CT. After administration of contrast medium, because of its predominant supply by the hepatic artery, the tumor shows arterial phase hyperenhancement, followed by rapid wash out on portal phase<sup>3,12,26</sup>.

If present, the tumor capsule appears as a hypodense rim on unenhanced images with enhancement in the delayed phase<sup>3,27,28</sup>.

**MRI:** HCC's appearance is generally heterogeneous on T1-weighted images because of the presence within the tumor of areas of haemorrhage, necrosis, fat and calcification. It mostly appears hyperintense on T2-weighted images<sup>15</sup>.

After administration of gadolinium, the tumor shows arterial phase hyperenhancement with rapid portal phase wash out.

If present, the tumor capsule appears hypointense on both T1-weighted and T2-weighted images with delayed enhancement after gadolinium administration<sup>3,27</sup>.

Using hepatospecific contrast agents in delayed post-contrast hepatobiliary phase MRI, HCC is usually hypointense<sup>8,12</sup>.

## **FIBROLAMELLAR CARCINOMA (FLC)**

### **Clinical features**

Fibrolamellar carcinoma (FLC) is a particular variant of HCC observed in adolescents and young adult patients. It arises in patients without chronic liver disease and there is no association with serum alpha-fetoprotein level<sup>12,29,30</sup>. Generally patients complain of abdominal pain or abdominal distension.

Usually fibrolamellar carcinoma presents itself as a solitary mass although in 10-15% of cases satellite lesions can be present<sup>12</sup>.

Typically it contains a central scar of myxoid tissue; in 68% of cases, there are calcifications within the lesion, usually located in the central scar<sup>29</sup>.

Metastasis in the loco-regional lymph nodes and intra-peritoneal spread are possible<sup>14</sup>. Other secondary sites of disease involvement are lungs and adrenal glands<sup>30</sup>.

## **Imaging features**

**US:** FLC appears as a circumscribed mass predominantly isoechoic or hyperechoic (Figure 8A), with a hyperechoic central scar possibly containing shadowing echogenic calcifications<sup>3</sup>.

**CT:** On unenhanced scan, FLC may appear isodense or hypodense to the adjacent liver. After contrast medium administration, tumor shows hyperenhancement during the arterial phase with variable attenuation during the portal venous phase (Figures 8B and 8C). The central scar is hypodense to the rest of the tumor, showing enhancement on delayed phase acquisitions<sup>30</sup>; in our experience, these imaging features resemble those of adult patients.

**MRI:** FLC is slightly hypointense on T1-weighted images and slightly hyperintense on T2-weighted images<sup>21</sup>. The central scar is typically hypointense on T2-weighted acquisitions and that is the most important feature for the differential diagnosis with FNH<sup>12</sup>.

After gadolinium administration, the tumor enhances more than adjacent liver. The central scar shows lack of enhancement during arterious and venous phases but a partial enhancement is seen on delayed phases<sup>21</sup>.

## **UNDIFFERENTIATED EMBRYONAL SARCOMA (UES)**

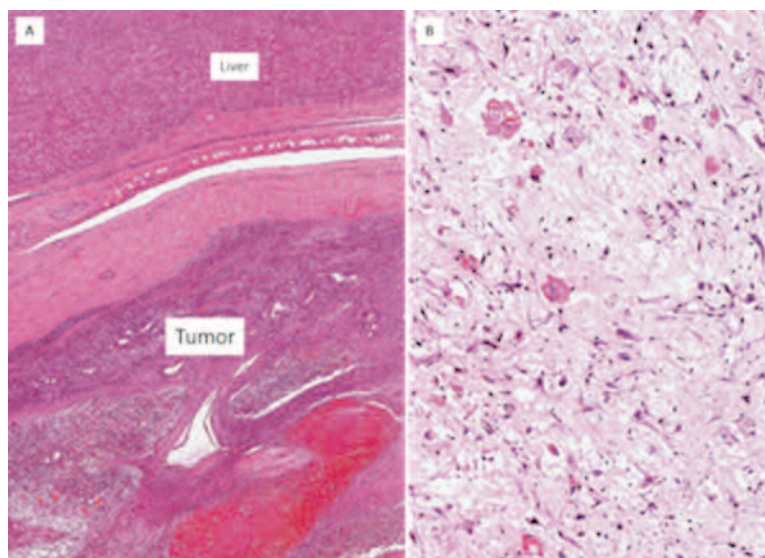
### **Clinical features**

Undifferentiated sarcoma of the liver is the third commonest malignant liver tumor in children and it represents less than 5% of all pediatric malignant liver tumors<sup>31,32</sup>. It was first described in 1978 by Stocker and Ishak<sup>33</sup>. It is an aggressive tumor of mesenchymal origin mostly diagnosed in children 6-10 years of age with a slight male predominance<sup>3</sup>; about 88% has been reported in children less than 15 years in age<sup>34</sup>. At the beginning, the prognosis was considered poor, with a median survival of less than one year. However, since the late 1980s long-term survivors were reported, due to chemotherapy performed before surgical resection<sup>34-36</sup>. The most common presenting symptom are abdominal pain, weight loss, fever and weakness<sup>37</sup>. Laboratory liver function tests and alpha-fetoprotein are usually normal<sup>37,38</sup>.



**Figure 8.** A case of fibrolamellar HCC in a 12-year-old child. US exam (A) demonstrates a predominantly isoechoic mass, containing small hyperechoic central foci. The lesion shows heterogeneous enhancement on arterial phase (B); a slight wash-out is observed on delayed phase (C) image.

**Figure 9.** Undifferentiated sarcoma: A, Neoplastic proliferation is separated from the normal liver by a thick fibrous pseudocapsule (haematoxylin and eosin, original magnification, x60). B, Higher magnification showing large atypical, spindle to stellate-shaped cells with hyperchromatic nuclei, set in a myxoid stroma. Some cells contain in their cytoplasm numerous eosinophilic globules of various sizes. This latter finding is frequently encountered in this tumor (haematoxylin and eosin, original magnification x 150).



UES usually presents itself as a solitary well demarcated large mass with a fibrous pseudocapsule (Figure 9). Metastases can involve the lung, pleura and peritoneum. Rare complications are spontaneous liver rupture and abdominal haemorrhage<sup>39</sup>.

### Imaging features

Imaging shows a heterogeneous mass with septa, necrosis, and haemorrhagic areas<sup>37</sup>.

US: UES appears as a solid isoechoic or hyperechoic mass (Figure 10) with small anechoic spaces corresponding to foci of necrosis, old haemorrhage or cystic degeneration<sup>3</sup>.

CT: Abdominal CT usually reveals the presence of a large well-circumscribed mass, with hypodense appearance (Figure 11)<sup>40,41</sup>. Unlike its solid ultrasound appearance, on CT scan UES shows a predominantly fluid aspect with internal septa and peripheral rim of enhancement on delayed images after administration of contrast

medium, corresponding to the fibrous pseudocapsule<sup>3,39,41</sup>. However, also homogeneous enhancement has been reported in literature<sup>42</sup>.

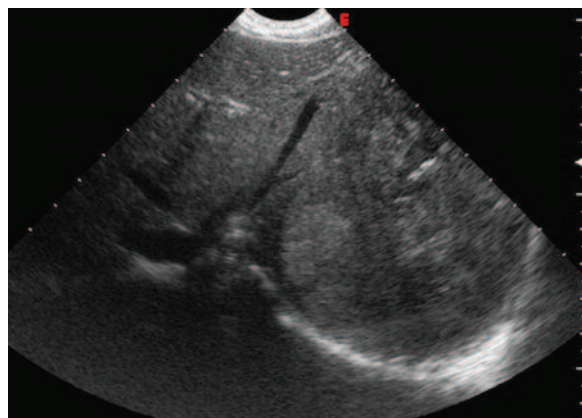


**Figure 10.** Imaging of same patient in Figure 9. On US images, the undifferentiated embryonal sarcoma appears as a large heterogeneous mass, with small anechoic and hyperechoic areas.

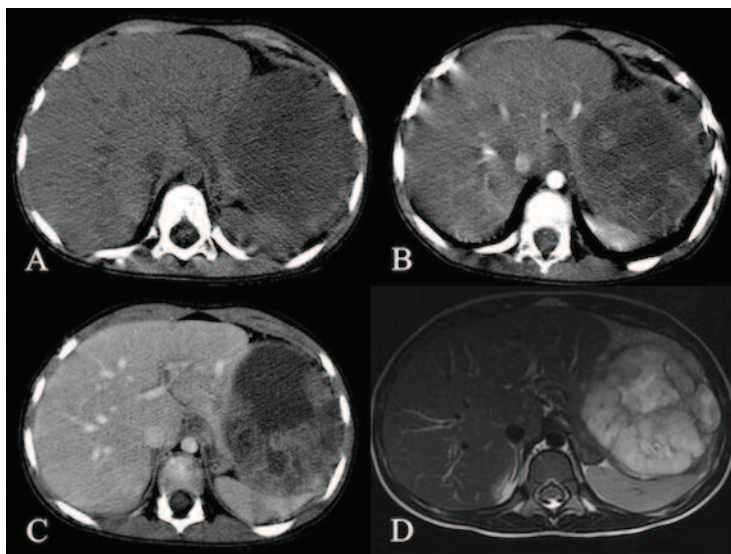


**Figure 11.** A case of undifferentiated embryonal sarcoma in a 3-year-old female (same patient in Figures 9-10). Unenhanced CT (A) shows a large well-circumscribed mass in the left hepatic lobe, with a predominantly fluid aspect. After contrast injection, on arterial phase (B) and delayed phase (C) images, the internal septa and the solid fibrotic parts demonstrate progressive enhancement, with a heterogeneous pattern. On T2-weighted-image (D), the lesion appears hyperintense with hypointense fibrotic pseudocapsule and internal septa.

Discrepancy of internal architecture on US and CT could be considered a very useful diagnostic marker to differentiate UES from other hepatic masses<sup>41</sup>.

MRI: UES appears hypointense on T1-weighted and hyperintense on T2-weighted images (Figure 11)<sup>40</sup>; focal areas of haemorrhage appear hyperintense on T1-weighted images and hypointense on T2-weighted images. After gadolinium administration, intralésional nodules could enhance, showing hyperintense signal. The fibrotic pseudocapsule is hypointense on both T1-weighted and T2-weighted images<sup>3</sup>.

Fluid-content, depicted both on CT and MR images, requires a careful differentiation from hydatidic cyst and liver abscess<sup>43,44</sup>.

## RHABDOMYOSARCOMA

### Clinical features

Liver rhabdomyosarcoma arises mostly in males, representing 1% of all liver tumors in childhood<sup>3,14</sup>.

Histologically, it has been differentiated into four types: pleomorphic, alveolar, embryonal and botryoidal<sup>45</sup>. Pleomorphic rhabdomyosarcoma is most frequent in adults, whereas embryonal type has been reported more commonly in infants and children<sup>45</sup>. Botryoid rhabdomyosarcoma is generally indicated also as “rhabdomyosarcoma of the biliary tract”.

This tumor usually shows itself as right upper abdominal mass with symptoms related to visceral compression, jaundice, fever, anorexia or vomiting, lethargy or malaise; however, its onset could be insidious, often represented only by aspecific symptoms such as anorexia and generalized weakness<sup>46</sup>. Less frequently, more or less in 17% of patients, it presents with spontaneous rupture of the tumor.

Alpha-fetoprotein is usually within normal range, LDH levels are very elevated and an elevation of predominantly conjugated bilirubin and alkaline phosphatase is also possible<sup>3,14</sup>. Metastatic disease at diagnosis is visible in 30% of patients<sup>3</sup>.

### Imaging features

Radiological findings of rhabdomyosarcoma are various; usually, rhabdomyosarcoma of the biliary tract appears as a large hilar mass with biliary duct dilatation<sup>47-48</sup>.

US: Tumor appears as a single heterogeneous hypoechoic mass or multiple hypoechoic lesions separated by septa; biliary dilatation could also be appreciated.

CT: The CT pattern is variable and the mass can be hypo- or hyperdense on the unenhanced-images, sometimes with biliary dilatation<sup>48</sup>. After contrast injection, the lesion can demonstrate a heterogeneous globular enhancement, but sometimes there is no enhancement.

MR: On MRI, the tumor usually appears as a partially cystic lesion, hypointense on T1-weighted images and hyper-intense on T2-weighted acquisitions, simulating a choledochal cyst<sup>3</sup>.

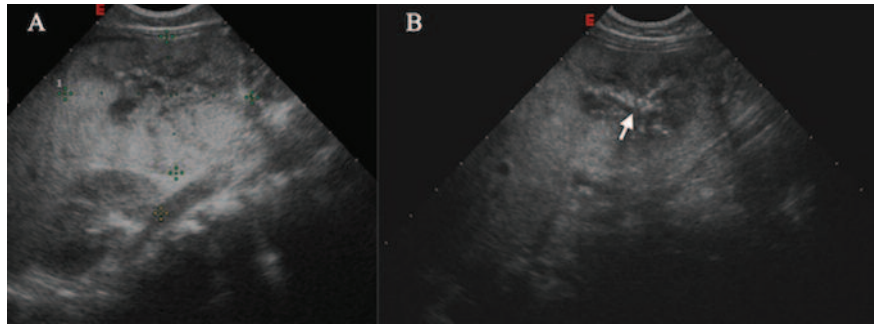
## EPITHELIOD HEMANGIOENDOTHELIOMA (EHE)

### Clinical features

Epithelioid hemangioendothelioma (EHE) is a rare neoplasm of vascular origin with intermediate malignant potential<sup>49</sup>. It most commonly affects females and it has an incidence of <0.1 per 100,000 population<sup>12,50</sup>. EHE grows slowly with a survival of 10 years in about 65% of patients<sup>51</sup>.



**Figure 12.** US findings of hemangioendothelioma in a 3-month-old child. The lesion appears mostly hypoechoic, with a heterogeneous central scar; small punctate calcifications are well depicted on B (white arrow).



Frequently this pathological entity is incidentally discovered because of its lack of symptoms<sup>3</sup>.

It can present with one or more liver lesions (nodular subtype), which are at the beginning located peripherally and can be associated with capsular retraction due to fibrotic reaction. Progressively lesions enlarge and coalesce to form confluent masses (diffuse subtype)<sup>12</sup>.

Metastases can involve lung, bone, lymph nodes, spleen and peritoneum<sup>3</sup>.

**Imaging features**

Imaging features of EHE are various; the most common appearance consists of multiple nodules in both hepatic lobes, simulating hepatic metastasis<sup>49</sup>. EHE often shows two radiological signs, useful to improve the diagnosis: “capsular retraction sign” due to fibrosis and “halo sign”, characterized by central hypodensity after intravenous contrast injection<sup>50</sup>. Usually, a biopsy is required for a correct diagnosis<sup>51</sup>.

US: US appearance of EHE is very heterogeneous but usually the tumor appears as a hypoechoic lesion near the liver capsule with irregular margins (Figure 12)<sup>3,51</sup>. Contrast Enhanced US is useful to

study the vascularization of the tumor; EHE shows a peripheral enhancement with a necrotic, haemorrhagic or scarred central avascular area<sup>51</sup>.

CT: On unenhanced images EHE appears hypodense. Multiphase CT demonstrates peripheral and progressive centripetal enhancement (Figure 13) with incomplete fill-in of larger lesions, while small lesions usually show central enhancement with centrifugal progression<sup>52</sup>.

MRI: EHE is usually hypointense on T1-weighted images and heterogeneously hyperintense on T2-weighted images<sup>3</sup>. According to Paoloantonio et al, other MRI findings are “ring or target enhancement” in the dynamic phases, lack of enhancement or “entrapment” in the hepatobiliary phase, and target appearance on DWI<sup>53</sup>.

**HEPATIC LYMPHOMA**

**Clinical features**

Primary hepatic lymphoma is a tumor confined to the liver without involvement of other lymphoid organs; it is extremely rare and it represents less than 1% of all extranodal lymphomas<sup>54,55</sup>. Primary liver lymphoma is usually a diffuse large B-cell

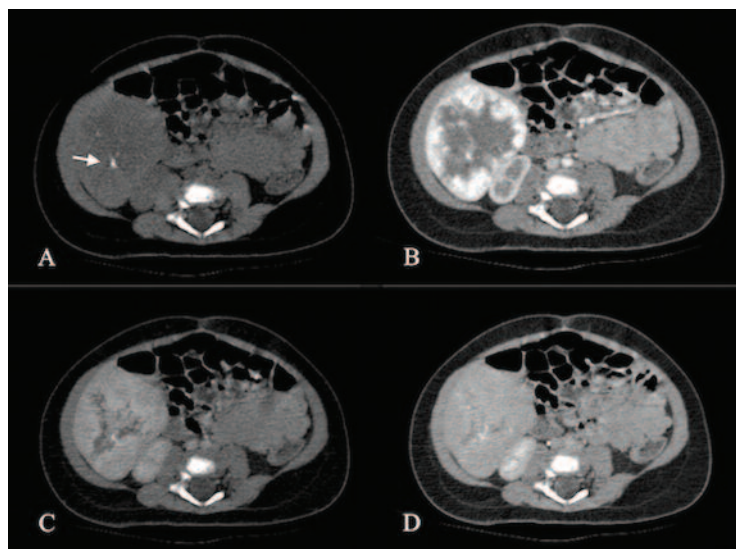


**Figure 13.** A case of hepatic hemangioendothelioma of the VI liver segment in a 3-month-old female (same patient in Figure 12). The lesion appears slightly hypodense with few calcific foci (white arrow) on unenhanced image (A). A progressive centripetal enhancement with almost complete fill-in is shown on the dynamic phases (arterial in figure B, portal in figure C and venous in D).

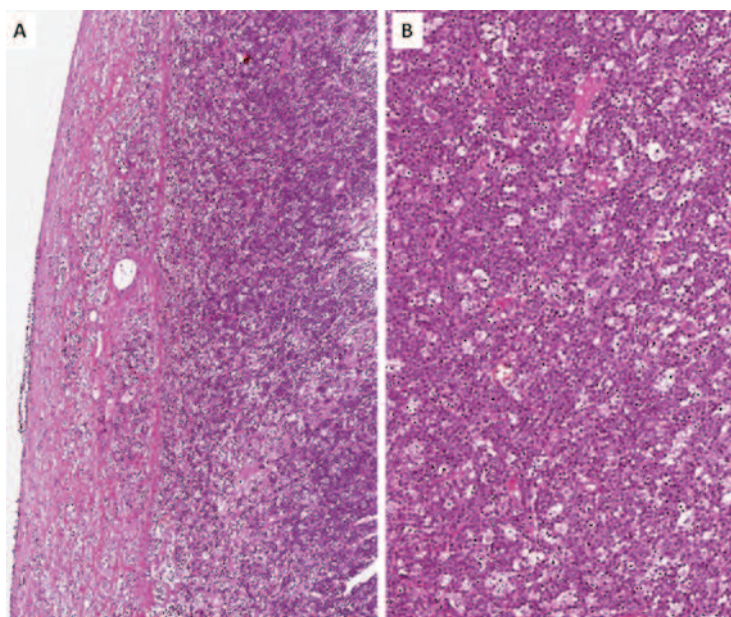


**Figure 14.** Burkitt lymphoma: A, neoplastic proliferation of round, medium-sized lymphoid cells, beneath the liver capsule (haematoxylin and eosin, original magnification, x80); B, the typical “starry sky” appearance is evident (haematoxylin and eosin, original magnification, x100). Diagnosis was confirmed by immunohistochemical analyses showing a diffuse CD20 positivity and Ki67 staining in >95% of neoplastic cells.

non-Hodgkin’s lymphoma affecting immunodeficient patients<sup>56</sup>. It is also considered in the spectrum of post-transplant lymphoproliferative disease, occurring in immunosuppressed individuals<sup>12</sup>. The diagnosis of primary liver lymphoma can be considered when a systemic lymphoproliferative disorder is excluded<sup>56</sup>. There are three morphological patterns of presentation: solitary nodule (60%), multiple focal nodules (35%) (Figure 14), and diffuse infiltrating without nodular formation (5%)<sup>55</sup>.

Symptoms are non specific and patients complain of abdominal pain and fever<sup>54</sup>.

### Imaging features

Imaging features of primary liver lymphoma are not pathognomonic and a definite diagnosis is often impossible.

US: The diffuse pattern of primary hepatic lymphoma is characterized by heterogeneous he-

patomegaly without any lesion<sup>55</sup>. Hypoechoic solitary or multiple nodules is shown in the nodular type (Figure 15)<sup>55</sup>.

CT: In the diffuse type, the liver shows a lower attenuation simulating hepatitis<sup>55</sup>. Solitary or multiple hypodense lesions characterize the nodular pattern (Figures 16); these lesions show a rim-like or slight enhancement in the arterial phase; in the portal venous and late phases, they appear hypodense<sup>57</sup>. Sometimes, CT features simulate liver metastasis from the gastrointestinal system<sup>54</sup>.

MRI: According to Coenegrachts et al<sup>56</sup>, the solitary pattern is characterized by a homogeneous lesion hypointense on T1-weighted images and hyperintense on T2-weighted images, without loss of signal in the “in and out of phase imaging”. After contrast administration, the nodule does not show any contrast enhancement in the arterial phase; in the late venous phase, it is slightly hyperintense and in delayed phases, the lesion is isointense with the liver parenchyma.

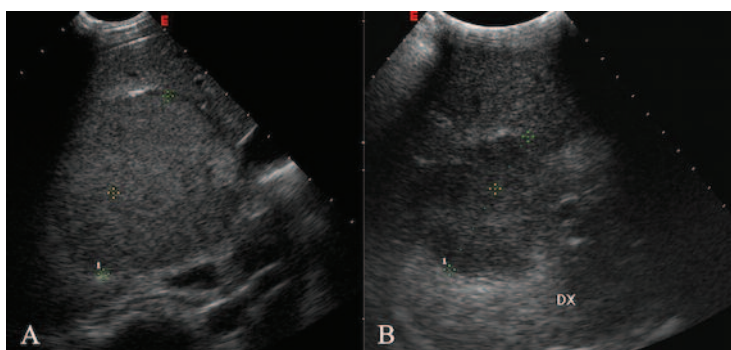
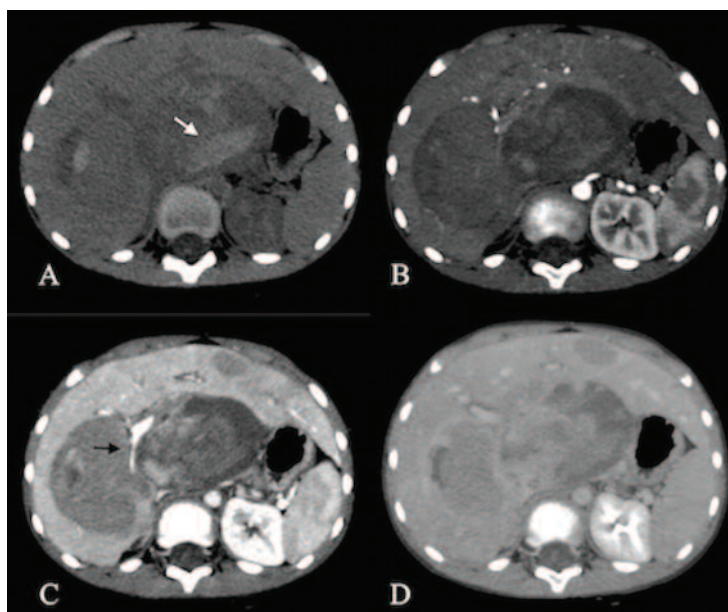


**Figure 15.** Primary hepatic lymphoma in a 13-year-old boy (same patient of histological samples in Figure 14), who was complaining of abdominal pain. US pattern is heterogenous, with a large, slightly hyperechoic mass on figure A, and a hypoechoic lesion on B.

**Figure 16.** Unenhanced (A) and dynamic (B-C-D) CT acquisition in a 13-year-old boy who was complaining of abdominal pain (same patient of Figures 14-15). On unenhanced image (A), two large isodense liver masses with hyperdense areas (white arrow) are shown, due to intra-lesional haemorrhage. In the arterial phase (B), lesions demonstrate a slight enhancement. On the portal venous (C) and delayed phases (D), these masses are hypodense to normal liver parenchyma; compression of portal veins is also shown (black arrow). The histological exam proved the diagnosis of primary hepatic lymphoma.



## ANGIOSARCOMA

### Clinical features

Angiosarcoma is a highly malignant tumor of vascular origin that represents 2% of all hepatic malignancy in children<sup>58</sup>. The prognosis is poor with a survival of about 5.5 months<sup>51</sup>; tumor behaviour is particularly aggressive<sup>59</sup>. It usually presents itself with hepatomegaly associated with non-specific symptoms, mainly represented by weight loss, anorexia, abdominal pain, fever, periumbilical tenderness and dyspnea<sup>3,60</sup>. Laboratory tests can show anemia, thrombocytopenia and consumptive coagulopathy; in 15-27% of patients symptoms are related to spontaneous tumor rupture with consequent hemoperitoneum. Metastases can involve lungs and spleen<sup>3</sup>.

### Imaging features

The tumor is generally multifocal, less frequently it shows up as a diffuse micronodular infiltration of the liver<sup>3</sup>.

US: Angiosarcoma usually appears as a heterogeneous mass with calcifications - hyperechoic foci with posterior acoustic shadowing foci<sup>30</sup>. Often, the lesion presents a heterogenous pattern, with some hyperechoic areas and hypoechoic nodules, which reflect respectively haemorrhage and necrosis<sup>60</sup>. It shows marked internal vascularity on Doppler evaluation<sup>21</sup>.

CT: Usually the nodules are hypoattenuating on unenhanced CT but they may contain hyperattenuating foci of acute haemorrhage. Lesions may

have irregular margins, very often not well markable from normal hepatic parenchyma. After administration of contrast medium, angiosarcomas mimic the peripheral nodular pattern with progressive centripetal fill-in of cavernous hemangioma<sup>60</sup>. However, complete centripetal fill-in is not seen because of the presence of central fibrosis or necrosis<sup>3</sup>.

MRI: Angiosarcomas are usually hypointense on T1-weighted images with possible hyperintense foci of acute haemorrhage. Tumors appear heterogeneously hyperintense on T2-weighted images with possible hypointense septa or fluid levels consistent with haemorrhage. Again, a hypertense signal may resemble the appearance of a hepatic hemangiomas. After administration of gadolinium, lesions show heterogeneous and irregular enhancement, without complete filling of central areas.

## METASTASES

Among pediatric patients, hepatic masses represent about 5-6% of all abdominal masses, and 0.5-2% are malignant<sup>61-62</sup>. Liver malignancies most frequently reported in children are metastases from neuroblastoma and Wilms' tumor<sup>61,63-64</sup>.

Neuroblastoma with liver metastases is associated with increased levels of urinary vanillylmandelic acid (VMA)<sup>65</sup>

Imaging features of neuroblastoma are not specific: liver involvement ranges from diffuse infiltration to multiple nodules<sup>61</sup>. Nodular lesions may be hypoechoic or hyperechoic at ultrasonography; on CT images, lesions are generally hypodense, with

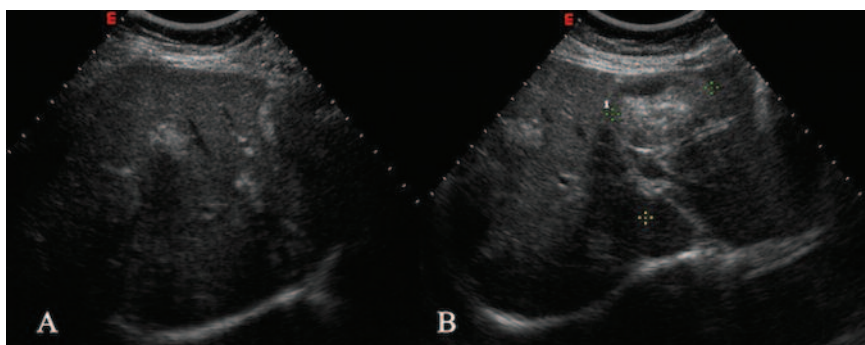


**Figure 17.** A case of 12-year-old female with a yolk sac tumor. On portal venous phase (A) and delayed phase (B) images, liver parenchyma shows multiple hypodense lesions in both hepatic lobes. These masses are referred to liver metastases.

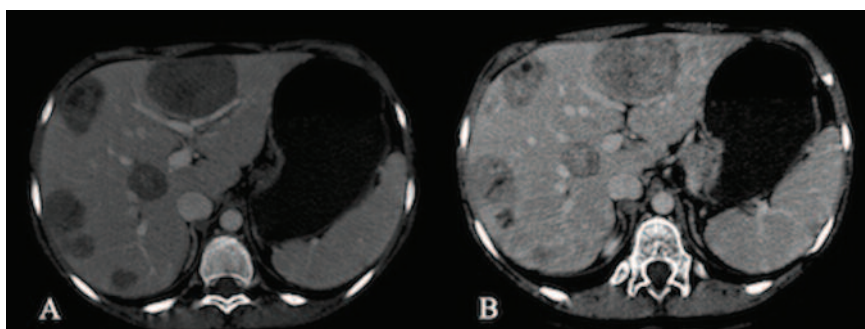


**Figure 18.** US examination in the same patient of Figure 17. Multiple hyperechoic masses are shown in both liver lobes.

lower enhancement than normal hepatic parenchyma<sup>61</sup>. MR imaging has been considered superior to CT in detecting hepatic metastases from neuroblastoma<sup>66</sup> at stage 4S, when liver parenchyma is characterized by diffuse metastatic infiltration.

Liver secondary lesions from Wilms' tumor have been reported as a poor prognostic factor; in addition, liver involvement at the diagnosis means "a worse prognosis than lung or other site of Stage IV disease"<sup>67</sup>. Lesions may appear hypodense on CT images, also in the dynamic phases after intravenous contrast administration; on MR imaging, they are generally hypointense on T1-weighted sequences and hyperintense on T2-weighted images, with lower enhancement after gadolinium administration<sup>21</sup>. This mentioned CT-MR imaging pattern is generally the most frequently encountered in case of hepatic metastases in infant and children (Figure 17); also US may show metastases in a non-specific pattern (Figure 18).

## CONCLUSIONS

Malignant primary liver tumors are characterized - in infants and children - by non-specific signs and symptoms, and radiological findings are often very useful in achieving a specific diagnosis and in staging and management. However, heterogeneity in appearance is more frequently observed using US, CT and MRI, making a differential diagnosis very hard.

## REFERENCES

1. Agarwala S, Jindal B, Jana M, Bhatnagar V, Gupta AK, Iyer VK. Malignant rhabdoid tumor of liver. *J Indian Assoc Pediatr Surg* 2014; 19: 38-40.
2. Keup CP, Ratnaraj F, Chopra PR, Lawrence CA, Lowe LH. Magnetic resonance imaging of the pediatric liver: benign and malignant masses. *Magn Reson Imaging Clin N Am* 2013; 21: 645-667.
3. Chung EM, Lattin GE Jr, Cube R, Lewis RB, Marichal-Hernández C, Shawhan R, Conran RM. From the archives of the AFIP: Pediatric liver masses: radiologic-pathologic correlation. Part 2. Malignant tumors. *Radiographics* 2011; 31: 483-507.
4. von Schweinitz D. Management of liver tumors in childhood. *Semin Pediatric Surg* 2006; 15: 17-24.
5. Roebuck DJ, Aronson D, Clapuyt P, Czauderna P, de Ville de Goyet J, Gauthier F, MacKinlay G, Maibach R, McHugh K, Olsen OE, Otte JB, Pariente D, Plaschkes J, Childs M, Perilongo G. International Childhood Liver Tumor Strategy Group. 2005 PRETEXT: a revised staging system for primary malignant liver tumours of childhood developed by the SIOPEL group. *Pediatr Radiol* 2007; 37: 123-132; quiz 249-250.
6. Rozell JM, Catanzano T, Polansky SM, Rakita D, Fox L. Primary liver tumors in pediatric patients: proper imaging technique for diagnosis and staging. *Semin Ultrasound CT MR* 2014; 35: 382-393.
7. Darge K, Anupindi SA, Jaramillo D. MR imaging of the abdomen and pelvis in infants, children, and adolescents. *Radiology* 2011; 261: 12-29.
8. Kolbe AB, Podberesky DJ, Zhang B, Towbin AJ. The impact of hepatocyte phase imaging from infancy to young adulthood in patients with a known or suspected liver lesion. *Pediatr Radiol* 2015; 45: 354-65.
9. MacKinlay GA, Pritchard J. A common language for childhood liver tumours. *Pediatr Surg Int* 1992; 7: 325-326.

10. Pritchard J, Brown J, Shafford E, Perilongo G, Brock P, Dicks-Mireaux C, Keeling J, Phillips A, Vos A, Plaschkes J. Cisplatin, doxorubicin, and delayed surgery for childhood hepatoblastoma: a successful approach – results of the first prospective study of the International Society of Pediatric Oncology. *J Clin Oncol* 2000; 18: 3819-3828.
11. Aronson DC, Schnater JM, Staalman CR, Weverling GJ, Plaschkes J, Perilongo G, Brown J, Phillips A, Otte JB, Czauderna P, MacKinlay G, Vos A. Predictive value of the pretreatment extent of disease system in hepatoblastoma: results from the International Society of Pediatric Oncology Liver Tumor Study Group SIOPEL-1 study. *J Clin Oncol* 2005; 23: 1245-1252.
12. Hegde SV, Dillman JR, Lopez MJ, Strouse PJ. Imaging of multifocal liver lesions in children and adolescents. *Cancer Imaging* 2013; 12: 516-529.
13. Roebuck DJ. Assessment of malignant liver tumors in children. *Cancer Imaging* 2009; 9 Spec No A: S98-S103.
14. Agarwala S. Primary Malignant Liver Tumors in Children. *Indian J Pediatr* 2012; 79: 793-800.
15. Helmberger TK, Ros PR, Mergo PJ, Tomczak R, Reiser MF. Pediatric liver neoplasms: a radiologic-pathologic correlation. *Eur Radiol* 1999; 9: 1339-1347.
16. Marino S, Caruso M, Magro G, D'Amico S, La Spina M, Moscheo C, Russo G, Di Cataldo A. Hepatoblastoma presenting as precocious puberty: a case report. *J Pediatr Endocrinol Metab* 2015; 28: 429-432.
17. Stocker JT. Hepatic tumors in children. *Clin Liver Dis* 2001; 5: 259-281, viii-ix.
18. de Campo M, de Campo JF. Ultrasound of primary hepatic tumours in childhood. *Pediatric Radiology* 1988; 19: 19-24.
19. Miller JH. The ultrasonographic appearance of cystic hepatoblastoma. *Radiology* 1981; 138: 141-143.
20. Dachman AH, Pakter RL, Ros PR, Fishman EK, Goodman ZD, Lichtenstein JE. Hepatoblastoma: radiologic-pathologic correlation in 50 cases. *Radiology* 1987; 164: 15-19.
21. Adeyiga AO, Lee EY, Eisenberg RL. Focal hepatic masses in pediatric patients. *AJR Am J Roentgenol* 2012; 199: W422-440.
22. Meyers AB, Towbin AJ, Geller JI, Podberesky DJ. Hepatoblastoma imaging with gadoxetate disodium-enhanced MRI—typical, atypical, pre- and post-treatment evaluation. *Pediatr Radiol* 2012; 42: 859-866.
23. Meyers AB, Towbin AJ, Serai S, Geller JI, Podberesky DJ. Characterization of pediatric liver lesions with gadoxetate disodium. *Pediatr Radiol* 2011; 41: 1183-1197.
24. Ni YH, Chang MH, Hsu HY, Hsu HC, Chen CC, Chen WJ, Lee CY. Hepatocellular carcinoma in childhood. Clinical manifestations and prognosis. *Cancer* 1991; 68: 1737-1741.
25. Kutluk T, Yalcin B, Ekinci S, Kale G, Akyuz C, Aydin B, Varan A, Demir HA, Buyukpamukcu M. Primary liver tumor in children: Hacettepe experience. *Turk J Pediatr* 2014; 56: 1-10.
26. Vu TL, Qureshi W, Turan N, Yonkers S, Stallings C, Semelka RC. *Applied Radiology* 2010; 39: 8-19.
27. Yu SC, Yeung DT, So NM. Imaging features of hepatocellular carcinoma. *Clin Radiol* 2004; 59: 145-156.
28. Palmucci S. Focal liver lesions detection and characterization: The advantages of gadoxetic acid-enhanced liver MRI. *World J Hepatol* 2014; 6: 477-485.
29. Ichikawa T, Federle MP, Grazioli L, Madariaga J, Nalesnik M, Marsh W. Fibrolamellar hepatocellular carcinoma: imaging and pathologic findings in 31 recent cases. *Radiology* 1999; 213: 352-361.
30. Pedrassa BC, da Rocha EL, Kierszenbaum ML, Bormann RL, Torres LR, D'Ippolito G. Uncommon hepatic tumors: iconographic essay - Part 1. *Radiol Bras* 2014; 47: 310-316.
31. Merli L, Mussini C, Gabor F, Branchereau S, Martelli H, Pariente D, Guérin F. Pitfalls in the Surgical Management of Undifferentiated Sarcoma of the Liver and Benefits of Preoperative Chemotherapy. *Eur J Pediatr Surg* 2015; 25: 132-137.
32. Ismail H, Dembowska-Baginska B, Broniszczak D, Kalincinski P, Maruszewski P, Kluge P, Swieszkowska E, Kosciesza A, Lembas A, Perek D. Treatment of undifferentiated embryonal sarcoma of the liver in children—single center experience. *Journal of Pediatric Surgery* 2013; 48: 2202-2206.
33. Stocker JT, Ishak KG. Undifferentiated (embryonal) sarcoma of the liver: report of 31 cases. *Cancer* 1978; 42: 336-348.
34. Baron PW, Majlessipour F, Bedros AA, Zuppan CW, Ben-Youssef R, Yanni G, Ojogho ON, Concepcion W. Undifferentiated embryonal sarcoma of the liver successfully treated with chemotherapy and liver resection. *J Gastrointest Surg* 2007; 11: 73-75.
35. Babin-Boilletot A, Flamant F, Terrier-Lacombe MJ, Marsden HB, van Unnik A, Deméocq F, Zucker JM, Voûte PA, Otten J, Behar C, Valayer J. Primitive malignant non-epithelial hepatic tumors in children. *Med Pediatr Oncol* 1993; 21: 634-639.
36. Kadomatsu K, Nakagawara A, Zaizen Y, Nagoshi M, Tsuneyoshi M, Fukushige T, Haigou A, Suita S. Undifferentiated (embryonal) sarcoma of the liver: report of three cases. *Surg Today* 1992; 22: 451-455.
37. Chocarro G, Amesty MV, Hernández F, Chenu BG, Ortiz R, Hernández S, Sánchez A, Gámes M, Santamaria ML, Tovar JA. Embryonal sarcoma of the liver. *Pediatr Surg Int* 2013; 29: 1261-1266.
38. Iqbal K, Xian ZM, Yuan C. Undifferentiated liver sarcoma – rare entity: a case report and review of the literature. *J Med Case Rep* 2008; 2: 20.
39. Küpeli S, Yalçın B, Çil BE, Akçören Z, Büyükpamukçu M. Undifferentiated embryonal sarcoma of the liver in a child complicated by haemorrhage. *Pediatr Radiol* 2008; 38: 1259-1261.
40. Crider MH, Hoggard E, Manivel JC. Undifferentiated (embryonal) sarcoma of the liver. *Radiographics* 2009; 29: 1665-1668.
41. Moon WK, Kim WS, Kim IO, Yeon KM, Yu IK, Choi BI, Han MC. Undifferentiated embryonal sarcoma of the liver: US and CT findings. *Pediatr Radiol* 1994; 24: 500-503.
42. Gondu GR, Eppa VR, Sowdepalli A, Narasimhan M, Ardhanari R. A rare case of childhood undifferentiated embryonal sarcoma of the liver managed successfully. *ACG Case Rep J* 2014; 1: 74-75.
43. Halefoglu AM, Oz A. Primary undifferentiated embryonal sarcoma of the liver misdiagnosed as hydatid cyst in a child: a case report and review of the literature. *JBR-BTR*. 2014; 97: 248-250.
44. Hanafiah M, Yahya A, Zuhdi Z, Yaacob Y. A case of an undifferentiated embryonal sarcoma of the liver mimicking a liver abscess. *Sultan Qaboos Univ Med J* 2014; 14: e578-581.
45. Rajamahendran R, Amudhan A, Prabhakaran R, Kannan D, Chandramohan SM. Embryonal rhabdomyosarcoma of liver in a 16-year-old boy: A rare case report. *Int J Hepatobiliary Pancreat Dis* 2014; 4: 52-56.
46. Haider N, Nadim MS, Piracha MN. Primary embryonal rhabdomyosarcoma of the liver in a young male. *J Coll Physicians Surg Pak*. 2013; 23: 750-751.



47. Friedburg H, Kauffmann GW, Böhm N, Fiedler L, Jobke A. Sonographic and computed tomographic features of embryonal rhabdomyosarcoma of the biliary tract. *Pediatr Radiol* 1984; 14: 436-438.
48. Donnelly LF, Bisset GS 3rd, Frush DP. Diagnosis please. Case 2: Embryonal rhabdomyosarcoma of the biliary tree. *Radiology* 1998; 208: 621-623.
49. Choi KH, Moon WS. Epithelioid hemangioendothelioma of the liver. *Cli Mol Hepatic* 2013; 19: 315-319.
50. Neofytou K, Chrysochos A, Charalambous N, Dietis M, Petridis C, Andreou C, Petrou A. Hepatic epithelioid hemangioendothelioma and the danger of misdiagnosis: report of a case. *Case Rep Oncol Med* 2013; 2013: 243939.
51. Schweitzer N, Soda B, Gebel M, Manns MP, Boozari B. Gray scale and contrast-enhanced ultrasound imaging of malignant liver tumors of vascular origin. *United European Gastroenterol J* 2015; 3: 63-71.
52. Chen Y, Yu RS, Qiu LL, Jiang DY, Tan YB, Fu YB. Contrast-enhanced multiple-phase imaging features in hepatic epithelioid hemangioendothelioma. *World J Gastroenterol* 2011; 17: 3544-3553.
53. Paolantonio P, Laghi A, Vanzulli A, Grazioli L, Morana G, Ragozzino A, Colagrande S. MRI of hepatic epithelioid hemangioendothelioma (HEH). *J Magn Reson Imaging* 2014; 40: 552-558.
54. Pedrassa BC, da Rocha EL, Kierzenbaum ML, Bormann RL, Francisc VV, D'Ippolito G. Uncommon hepatic tumors: iconographic essay - Part 2. *Radiol Bras* 2014; 47: 374-379.
55. Lu Q, Zhang H, Wang WP, Jin YJ, Ji ZB. Primary non-Hodgkin's lymphoma of the liver: sonographic and CT findings. *Hepatobiliary Pancreat Dis Int* 2015; 14: 75-81.
56. Coenegrachts K, Vanbeckevoort D, Deraedt K, Van Steenberghe W. Mri findings in primary non-Hodgkin's lymphoma of the liver. *JBR-BTR* 2005; 88: 17-19.
57. Maher MM, McDermott SR, Fenlon HM, Conroy D, O'Keane JC, Carney DN, Stack JP. Imaging of primary non-Hodgkin's lymphoma of the liver. *Clin Radiol* 2001; 56: 295-301.
58. Fernandez-Pineda I, Cabello-Laureano R. Differential diagnosis and management of livers in infants. *World J Hepatol* 2014; 6: 486-495.
59. Litten JB, Tomlinson GE. Liver tumors in children. *Oncologist* 2008; 13: 812-820.
60. Emre S, McKenna GJ. Liver tumors in children. *Pediatr Transplantation* 2004; 8: 632-638.
61. Rivard DC, Lowe LH. Radiological reasoning: multiple hepatic masses in an infant. *AJR Am J Roentgenol* 2008; 190(6 Suppl): S46-52.
62. Davey MS, Cohen MD. Imaging of gastrointestinal malignancy in childhood. *Radiol Clin North Am* 1996; 34: 717-742.
63. Cohen MD, Siddiqui A. Liver metastases in Wilms' tumour. *Clin Radiol*. 1982; 33: 539-40.
64. David R, Lamki N, Fan S, Singleton EB, Eftekhari F, Shirkhoda A, Kumar R, Madewell JE. The many faces of neuroblastoma. *Radiographics* 1989; 9: 859-82.
65. Bond JV. Neuroblastoma metastatic to the liver in infants. *Arch Dis Child* 1976; 51: 879-882.
66. Nour-Eldin NE, Abdelmonem O, Tawfik AM, Naguib NN, Klingebiel T, Rolle U, Schwabe D, Harth M, El-toukhy MM, Vogl TJ. Pediatric primary and metastatic neuroblastoma: MRI findings: pictorial review. *Magn Reson Imaging* 2012; 30: 893-906.
67. Ehrlich PF, Ferrer FA, Ritchey ML, Anderson JR, Green DM, Grundy PE, Dome JS, Kalapurakal JA, Perlman EJ, Shamberger RC. Hepatic metastasis at diagnosis in patients with Wilms tumor is not an independent adverse prognostic factor for stage IV Wilms tumor: a report from the Children's Oncology Group/National Wilms Tumor Study Group. *Ann Surg* 2009; 250: 642-648.